Godoy-Reyes, TM.; Costero, AM.; Gaviña, P.; Martínez-Máñez, R.; Sancenón Galarza, F. (16-0). Colorimetric detection of normetanephrine, a pheochromocytoma biomarker, using bifunctionalised gold nanoparticles. Analytica Chimica Acta. 1056:146-152. https://doi.org/10.1016/j.aca.2019.01.003

Colorimetric detection of normetanephrine, a pheochromocytoma biomarker, using bifunctionalised gold nanoparticles

Tania M. Godoy-Reyes,[a,b,d] Ana M. Costero,[a,b,c] Pablo Gaviña,[a,b,c,*] Ramón Martínez-Máñez,[a,b,d,*] and Félix Sancenón[a,b,d]

[a] Instituto Interuniversitario de Investigación de Reconocimiento Molecular y Desarrollo Tecnológico (IDM), Universitat Politècnica de València, Universitat de València, Spain
[b] CIBER de Bioingeniería, Biomateriales y Nanomedicina (CIBER-BBN), Spain
[c] Departamento de Química Orgánica, Universitat de València, Doctor Moliner 50, Burjassot, 46100, Valencia, Spain
[d] Departamento de Química, Universitat Politècnica de València, Camino de Vera s/n, 46022, Valencia, Spain
* Corresponding authors. E-mail addresses: pablo.gavina@uv.es (P. Gaviña), rmaez@qim.upv.es (R. Martínez-Mañez).

Abstract: A simple and effective colorimetric method for the detection of normetanephrine (NMN), an *O*-methylated metabolite of norepinephrine, using functionalised gold nanoparticles is described. This metabolite is an important biomarker in the diagnosis of adrenal tumours such as pheocromocytoma or paraganglioma. The colorimetric probe consists of spherical gold nanoparticles (AuNPs) functionalized with two different ligands, which specifically recognize different functional groups in normetanephrine. Thus, a benzaldehyde-terminated ligand was used for the recognition of the amino alcohol moiety in NMN, by forming the corresponding oxazolidine. On the other hand, *N*-acetyl-cysteine was chosen for the recognition of the phenolic hydroxyl group through the formation of hydrogen bonds. The selective double molecular recognition between the probe and the hydroxyl and the amino-alcohol moieties of normetanephrine led to interparticle-crosslinking aggregation resulting in a change in the color of the solution, from red to blue, which could be observed by naked eye. The probe was highly selective towards normetanephrine and no color changes were observed in the presence of other neurotransmitter metabolites such as homovanillic acid (HVA) (dopamine metabolite), 5-hydroxyindoleacetic acid (5-HIAA) (serotonin metabolite), or other biomolecules present in urine such as glucose (Glc), uric acid (U.A), and urea. Finally, the probe was evaluated in synthetic urine with constituents that mimic human urine, where a limit of detection of 0.5 µM was achieved.

Keywords: Normetanephrine • gold nanoparticles • colorimetric detection • aggregation • pheocromocytoma

1. Introduction

Normetanephrine (NMN) is an *O*-methylated metabolite of norepinephrine produced by the enzyme catechol-*O*-methyltransferase within tumours. This metabolite is one of the most useful biomarkers for the early diagnostic of neuroendocrine tumours such as pheochromocytomas and paragangliomas (PPGL) [1-3]. These tumours, which cause hypertension and occur with headaches, excessive sweating and palpitations, arise from the intra-adrenal and extra-adrenal chromaffin cells, and are characterized by an overproduction of catecholamines, which result in increased levels of their *O*-methylated metabolites in plasma or urine, being NMN the metabolite found in the highest concentration [4]. Measurements of NMN levels in plasma or urine are recommended for first line biochemical diagnosis of PPGL [5-6].

Some analytical methods such as electrochemistry [7], radioimmunoassays [8-9], enzyme-linked immunosorbent assay (ELISA) [10], high performance liquid chromatography with tandem mass spectrometry (HPLC-MS) [11-14] with fluorogenic detection (HPLC-FD) [15-16] and with electrochemical detection (HPLC-ED)[17-19] have been developed for the quantification of NMN in human plasma and urine. However, the application of these techniques requires of sophisticated and expensive equipment, in addition to their complicated sample-preparation and professional operation. Due to the limitations of the above-mentioned analytical methods and the importance of the determination of NMN for the diagnosis of PPGL, the development of simple analytical techniques that can be readily applied to the measurement of NMN in clinical samples is of high interest. Colorimetric probes are especially appealing as sensing devices because there are few techniques as simple as visual detection and they allow rapid and sensitive determination to the naked eye, on site, without any sample pre-treatment. However, to the best of our knowledge, the only colorimetric assay for NMN detection is based on the Pisano colorimetric method, which measures the total content of metanephrines (normetanephrine and metanephrine) in urine, after their conversion into vanillin through oxidation using periodate. This method is non-specific, and involves lengthy separations and sample pre-treatment [20-22].

In recent years, spherical gold nanoparticles have received great attention as platforms in the development of colorimetric sensors and probes. AuNPs have wonderful optoelectronics properties [23-24]. In particular the surface plasmon resonance (SPR) band, which can be modified upon the analyte–induced aggregation of the nanoparticles. This modification in the SPR band results in a color change from red (dispersed AuNPs) to blue (aggregated AuNPs) which

can be observed by naked eye. Other great advantages are their good biocompatibility and ease of surface functionalisation with different organic molecules. Thus, numerous selective and sensitive colorimetric probes based on functionalised AuNPs, which allow the selective determination of different types of analytes at very low concentrations, have been reported [25-28].

Taking into account the above mentioned facts, we present herein a novel approach for the fast, simple and selective determination of normetanephrine in water and in simulated urine, based on the use of bifunctionalised gold nanoparticles. Probe **GNP1** consists of spherical gold nanoparticles functionalised with two different moieties: a benzaldehyde-terminated ligand (**L1**) which can react with the aminoalcohol group of NMN to give the corresponding oxazolidine [29], and *N*-acetylcysteine (**L2**), which binds the phenolic hydroxyl group through the formation of hydrogen bonds, and is also a good stabilizer of gold nanoparticles due to its carboxylate group [30-31]. This double molecular interaction with NMN leads to aggregation of the nanoparticles, resulting in a strong bathochromic shift of their SPR band and a color change of the solution from red to blue, visible to the naked eye. The recognition approach is shown in Scheme 1 .

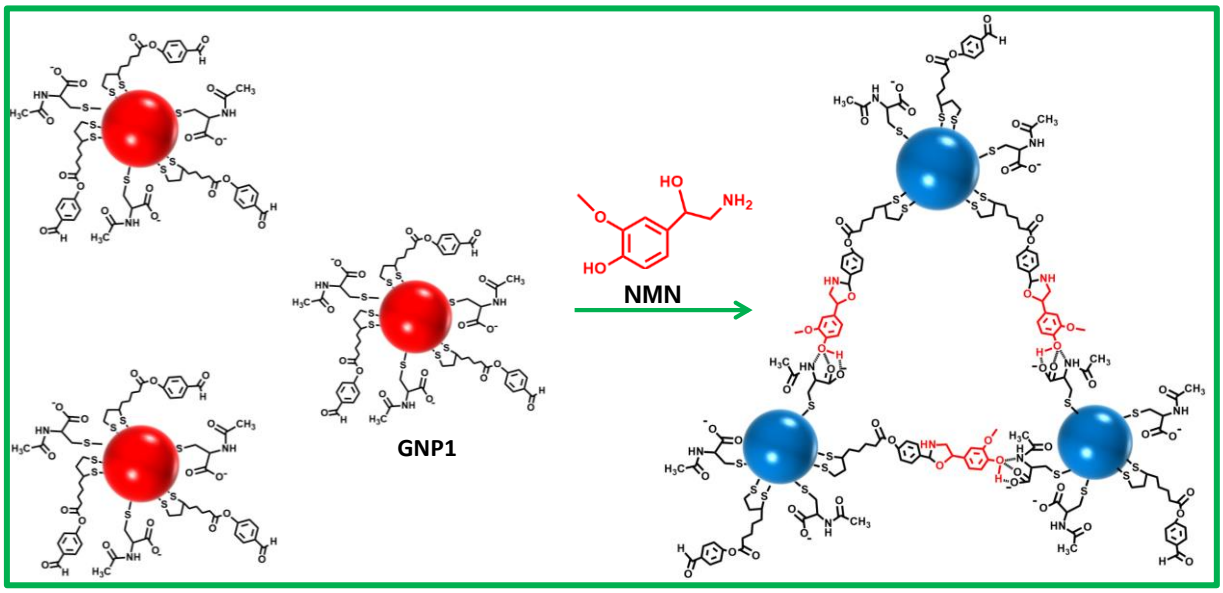

Scheme 1. Sensing paradigm of the colorimetric detection of normetanephrine (NMN) based on the aggregation of gold nanoparticles (**GNP1**) bifunctionalised with 4-(liponyloxy)benzaldehyde (**L1**) and N-acetylcysteine (**L2**).

2. Experimental

2.1. Chemicals

Gold (III) chloride hydrate ($HAuCl_4 \cdot 3H_2O$) 99.995%, sodium citrate dihydrate, *N-Acetyl-L-cysteine* ≥*99%* (**L2**), (±)-α-lipoic acid ≥98.0%, 4-hydroxybenzaldehyde 98%, *N,N'*-dicyclohexylcarbodiimide (DCC) 99%, 4-dimethylaminopyridine (DMAP) ≥99%, homovanillic acid (HVA) ≥99.0%, 5-Hydroxyindole-3-acetic acid (5-HIAA) ≥98%, D-(+)-Glucose (Glc) ≥99.5%, uric acid (U.A) ≥99%, urea 98% and surine negative urine, were purchased from Sigma Aldrich and used without further purification. All the aqueous solution were prepared with Mili-Q water (18.2 $M\Omega\ cm^{-1}$).

2.2. General Methods

UV-Vis absorption spectra were recorded using a 1 cm path length quartz cuvette on a Shimadzu UV-2101PC spectrophotometer. All measurements were carried out at room temperature. To characterize the induced aggregation of the gold nanoparticles probe in the presence of normetanephrine, high-resolution transmission electron microscopy (JEOL-1010 transmission electron microscopy operating at 100 kV) was used. Z potential and DLS values were measured in a Malvern Zetasizer ZS, for 3 times in 10-25 cycles. To verify the gold nanoparticles functionalization Fourier-transform infrared spectra were recorded with a Cary 630 FT-IR spectrometer within the wavenumber range of 648-4000 cm^{-1} at a resolution of 8 cm^{-1}. To confirm the structure of ligand L1 ^{1}H-NMR and ^{13}C-NMR spectra were recorded with a Bruker DRX-300 Spectrometer (300 MHz, 128 scans). Chemical shifts are reported in ppm with tetramethylsilane as an internal standard.

*2.3 Synthesis of 4-(liponyloxy)benzaldehyde (**L1**)*

4-(Liponyloxy)benzaldehyde (**L1**) was synthesized as previously reported [35] from (±)-α-lipoic acid (0.75 g, 3.63 mmol), 4-hydroxybenzaldehyde (0.44 g, 3.63 mmol), DCC (0.75 g, 3.63 mmol) and a catalytic amount of DMAP (0.04 g, 0.33 mmol) in anhydrous CH_2Cl_2 (10 mL). **L1** was obtained as a yellow oil in 86% yield.

^{1}H NMR (300 MHz, $CDCl_3$) δ 9.98 (s, 1H), 7.91 (d, J = 9.0, 2H), 7.26 (d, J = 9.0, 2H), 3.61–3.57 (m, 1H), 3.22 – 3.09 (m, 2H), 2.60 (t, J = 7.4 Hz, 2H), 2.51 – 2.42 (m, 1H), 1.97 – 1.88 (m, 1H), 1.84 – 1.67 (m, 4H), 1.63 – 1.52(m,2H). ^{13}C NMR (75 MHz, $CDCl_3$) δ 190.96, 171.71, 155.35, 134.39, 131.25, 122.51, 56.53, 40.51, 38.79, 34.94, 34.21, 28.64, 24.77.

*2.4 Synthesis of probe **GNP1***

First, citrate-coated AuNPs with a diameter ca. 17 nm were synthesized as reported previously [32-34]. Briefly, 5 mL of 13.6 mM aqueous trisodium citrate solution were added to an aqueous boiling solution of $HAuCl_4$ (95 mL, 0.23 mM) and the resulting mixture was kept continuously boiling for 30 min until a red solution was obtained. The solution was cooled to room temperature, and then the mixture was purified by filtration through a 0.22 µM membrane and the filtrate was then stored in a refrigerator at 4°C until use.

Probe **GNP1** was prepared from the previously synthesized citrate-capped AuNPs (ca. 17 nm) by a stepwise ligand-exchange reaction. Thus, 20 µl of **L2** 1 mM in DMF were added to 10 mL of the as-prepared citrate capped AuNPs. After stirring for 1 min at room temperature, 20 µl of **L1** 1 mM in DMF were added. The solution was stirred 5 h at room temperature. To purify **GNP1**, the mixture was centrifuged for 10 min at 11,000 rpm, the supernatants were decanted and the nanoparticles redispersed in Mili-Q water (10 mL). This procedure was repeated twice.

*2.5 Synthesis of probe **GNP2***

GNP2 nanoparticles were synthesized following the same procedure as **GNP1**. First, citrate-coated AuNPs of ca. 34 nm were prepared, following the process mentioned above, but in this case, using 5 mL of 3.4 mM aqueous trisodium citrate solution. Probe **GNP2** was obtained by the stepwise addition of **L2** and **L1** to the as-synthesized citrate-capped AuNPs using the same amounts and the same procedure as described above for GNP1.

2.6 Sensing and selectivity studies

For the UV-vis titration experiments, aqueous solutions of normetanephrine of different concentrations at pH 7 (phosphate buffer 10 mM) were freshly prepared. Then, 200 µL of **GNP1** (8.12×10^{-10} M) and 200 µL of the NMN solution at an appropriate concentration (0–24 mM) were mixed to obtain a final volume of 400 µL. As an example, 400 µL of a solution containing **GNP1** 4.06×10^{-10} M and NMN 5 mM were obtained by mixing 200 µL of **GNP1** and 200 µL of NMN 10 mM. Samples were incubated at room temperature for 6 min before recording the corresponding UV-vis spectra. The same procedure was followed to evaluate the sensing ability of **GNP2** (NMN final concentrations of 1, 6 and 10 mM). The selectivity studies were performed following the same procedure by mixing 200 µL of **GNP1** (8.12×10^{-10} M) and 200 µL of an aqueous buffered solution (pH = 7) of the studied interferent (10 mM). A competitive study was performed by adding 200 µL

of an aqueous buffered solution containing a mixture of NMN and all the interferents (10 mM each) to 200 µL of **GNP1**. The titration experiments with optimized probe (**OGNP1**) were conducted as follows: **OGNP1** was freshly prepared by adding 20 µL of NMN 80 mM to 200 µL of the **GNP1** solution, and incubating the mixture for 1 min at room temperature. Then, 180 µL of the NMN sample solution at an appropriate concentration (0–20 µM) were added to the **OGNP1** solution to obtain a final volume of 400 µL. Samples were incubated for 6 min before taking measurements in the spectrophotometer. Measurements in simulated urine were made using Surine™ Negative Urine Control, that is rugged non-biological urine with constituents that mimic human urine, but without human urine´s research impediments. In a typical experiment, 200 µL of **OGNP1** were mixed with 200 µL of NMN solutions in 20% Surine Negative Urine Control, incubated for 6 min, and analysed by UV-vis spectrophotometry.

3. Results and Discussion

3.1 *Synthesis and characterization of* ***GNP1***

Compound **L1** was obtained through Steglich esterification of lipoic acid with 4-hydroxybenzaldehyde using as a coupling agent DCC and DMAP as a catalyst [35]**.** On the other hand, citrate-capped AuNPs were prepared by the Turkevich-Frens method wich consist in the reduction of tetrachloroauric acid with trisodium citrate in boiling water [32-34]. Addition of **L1** and **L2** (1:1 molar ratio) to the citrate-stabilized AuNPs led to the formation of probe **GNP1** through ligand exchange reactions, due the highly stable S-Au interactions. The functionalised gold nanoparticles were purifed by repeated centrifugation and redispersion in water to yield a red colored solution.

Probe **GNP1** was characterized by UV-vis spectroscopy, transmission electron microscopy (TEM), dynamic light scattering (DLS) and infrared spectrospcopy (FTIR). The aqueous dispersions of **GNP1** showed the typical SPR band at 523 nm in the UV-vis spectrum, in accordance with the values observed for dispersed AuNPs with sizes smaller than 25 nm [36-37]. The average size of the nanoparticles turned out to be of 17 nm from TEM measurements (Figure S1 C). Regarding the hydrodynamic diameter of the dispersed nanoparticles DLS showed an increase from 28 nm for citrate-stabilized AuNPs to 30 nm for **GNP1** (Figure S2). The zeta-potential value of the **GNP1** nanoparticles in aqueous solution was -30.6 mV. Finally, the ligand exchange was confirmed by FTIR, showing bands characteristic of **L1** and **L2** (Figure S4). The concentration of **GNP1** probe

solution was calculated to be ca. 6 x 10^{-10} M by UV-vis spectroscopy considering an estimated molar extinction coefficient of ε = 6.01 x 10^{8} M^{-1} cm^{-1} [38]. The red colored aqueous dispersion of **GNP1** remained stable in the refrigerator for more than a month, with no observable changes in color nor in its SPR band. Furthermore, to evaluate the influence of the size of the nanoparticles in the sensitivity towards NMN, probe **GNP2** was prepared from citrate-capped AuNPs of ca. 34 nm and ligands **L1** and **L2** following the same procedure as for **GNP1**, resulting in stable red suspensions (see Supp. Info). Citrate-capped AuNPs of ca. 42 nm were also prepared. However, all attempts of functionalizing these nanoparticles with **L1** and **L2** resulted in their aggregation.

3.2 *Sensing ability of **GNP1** towards normetanephrine*

GNP1 sensing capabilities were evaluated in the absence and presence of NMN (5 mM) at pH 7 (phosphate buffer, 10 mM). In the absence of NMN the aqueous suspension of **GNP1** remained red with its characteristic SPR band at 523 nm in the UV-vis spectrum. However, in presence of excess NMN the red color changed progressively to blue within minutes, and the corresponding UV-vis spectrum showed a shift in the SPR band from 523 nm to 612 nm, indicating the aggregation of **GNP1** induced by NMN. This aggregation was further confirmed by TEM (Figure S1 A and B, corresponding to dispersed and aggregated nanoparticles) and DLS studies. The latter shows that in the presence of NMN the hydrodynamic radius of the particles increases from 30 nm to 450 nm (see Figure S3 A and B). The zeta potential reduced from -30.6 mV (**GNP1**) to -9.35 mV (**GNP1** + NMN). In addition, UV-vis kinetic studies confirmed a significant increase in the absorbance at 612 nm of **GNP1** in the presence of NMN, starting at the first minute, and reaching its maximum point approximately after 6 min (Figure S5).

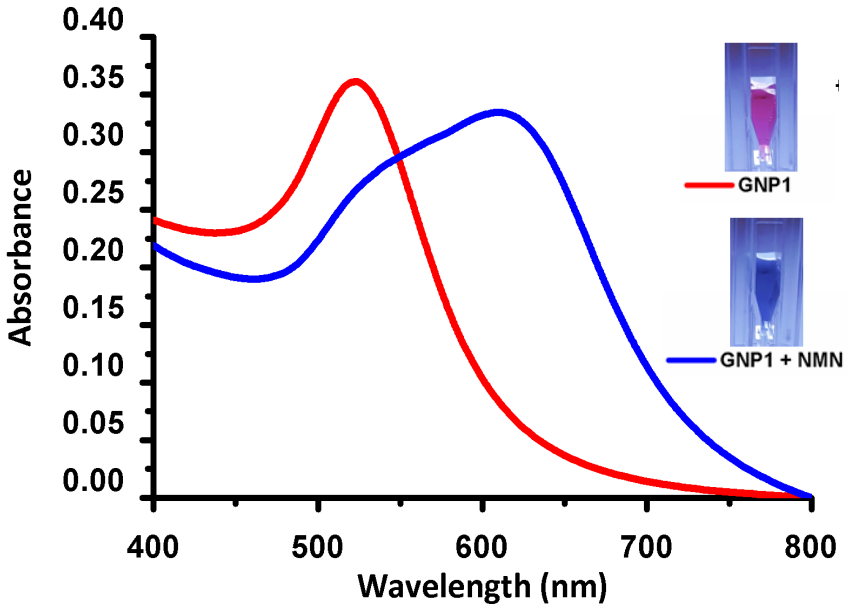

Figure 1. UV-Vis spectra of **GNP1** in the absence (red) and presence of NMN (5 mM) (blue) at pH 7 (phosphate buffer, 10 mM).

3.3 *Selectivity evaluation of **GNP1** in the presence of possible interferents*

Selective and sensitive detection of NMN plays a key role in the diagnosis of tumors such as pheochromocytoma. Selectivity features of **GNP1** were evaluated in presence of other neurotransmitter metabolites such as, homovanillic acid (HVA, a dopamine metabolite) and 5-hydroxyindoleacetic acid (5-HIAA, a serotonin metabolite), and other biomolecules present in urine such as glucose (Glc), uric acid (U.A) and urea. After the addition of excess (5 mM final concentration) of the potential interferents to **GNP1**, negligible changes in the A_{612}/A_{523} ratio (A_{612} = absorbance at 612 nm, A_{523} = absorbance at 523 nm), nor in the color of the solutions were observed (see Figure 2a and 2b and Figure S6). Moreover, in a competitive experiment, the addition of a mixture containing NMN and all the interferents (HVA, 5-HIIA, Glc, U.A and urea) to **GNP1** led to a response similar to that found when only NMN is added to **GNP1**, (Figure 2b). All these data indicate that **GNP1** is able to selectively detect NMN in aqueous media in the presence of other neurotransmitter metabolites and selected biomolecules.

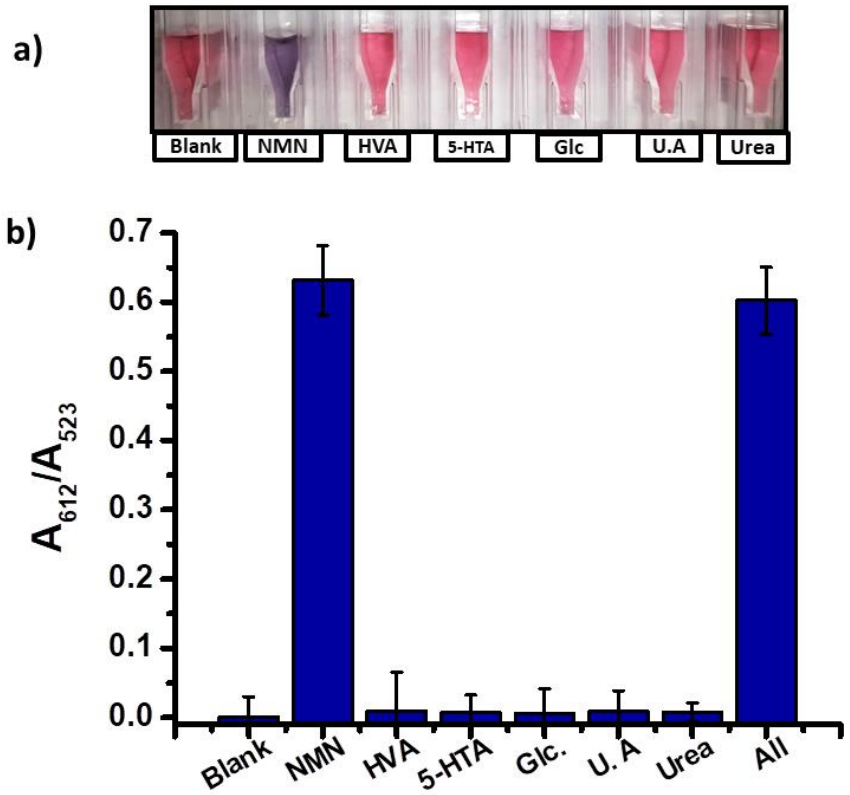

Figure 2. Response of **GNP1** in the presence of different molecules (5 mM) at pH 7 (phosphate buffer, 10 mM). a) Vials with the different tested molecules. b) Representation of A_{612}/A_{523} for NMN and the interferents. Error bars correspond to the s. d. from three independent experiments.

3.4 *Sensitivity studies and optimization of* ***GNP1***

In order to evaluate the influence of the size of the nanoparticles in the sensitivity, the response of **GNP1** (17 nm) and **GNP2** (34 nm) in front of NMN (1, 6 and 10 mM) was compared by UV-vis spectroscopy. As observed in Fig S8 and S9, **GNP1** showed a higher sensitivity than **GNP2**. Thus, all experiments were performed with **GNP1**. In order to determine the sensitivity of the response of **GNP1** towards NMN, UV-vis titration experiments in the presence of increasing concentrations of NMN (from 0 to 12 mM) were undertaken. As the concentration increased, a gradual change in the color of the nanoparticles is clearly observed, changing from red to purple and finally to blue (Figure 3a). Moreover as the amount of NMN increases a shift in the SPR band from 523 nm (dispersed nanoparticles) to 612 nm (aggregated) was observed by UV-vis (Figure 3b), confirming in this way the sensing protocol based on the NMN-induced aggregation of **GNP1**. As seen in Figure 4, a remarkable increase in the A_{612}/A_{523} ratio was observed in the 4–10 mM concentration range, indicating a higher sensitivity of the probe within these NMN concentration values. Consequently, the sensitivity of the probe towards NMN detection could be improved by the addition of certain amount of NMN (to yield a final concentration of 4 mM) to the stock solution of

GNP1 before use [39]. Figure 5 shows clearly how the sensitivity towards NMN of this optimized probe (**OGNP1**) increases with respect to the sensitivity of **GNP1** in the 0–10 µM range (Figure 5, curves a and b). The limit of detection (LOD), calculated from the plot of A_{612}/A_{523} vs NMN concentration in this low concentration range, was 4.7 µM for **GNP1**, and as low as 0.2 µM for **OGNP1**. This LOD confers our system a competitive basis for the detection of NMN at relevant clinical concentration. In particular, reported studies have determined that for normotensive patients, NMN levels above the normal range of 0.15 to 3.05 µM in urine can be indicative of pheochromocytoma and paraganglioma tumours [40].

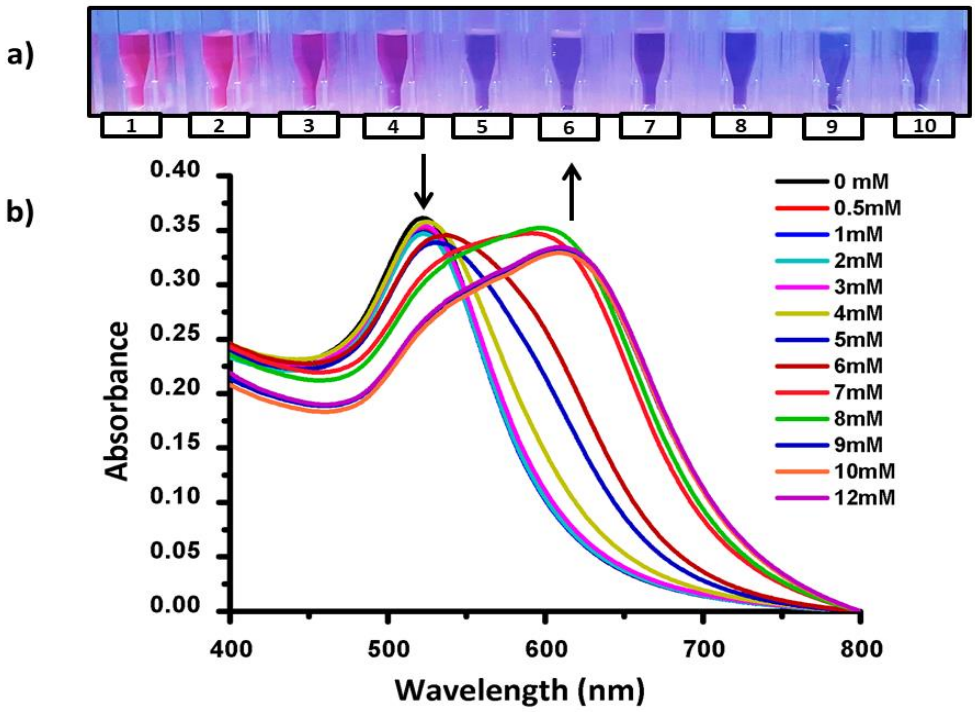

Figure 3. a) Colour modulation of **GNP1** when NMN was added at concentrations of 0, 3, 4, 5, 6, 7, 8, 9, 10, 11 mM (1-10, respectively). b) Changes in the UV-Vis spectra of probe when NMN was added at concentrations of 0, 0.5, 1, 2, 3, 4, 5, 6, 7, 8, 9, 10, 11, 12 mM

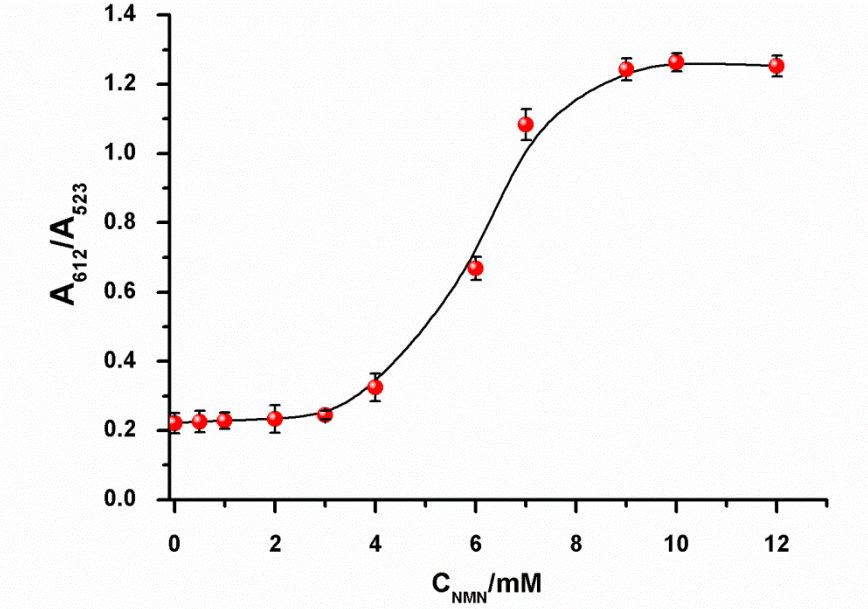

Figure 4. Plot of A_{612}/A_{523} versus NMN concentration (0-12 mM) obtained with **GNP1**. Error bars correspond to the s. d. from three independent experiments.

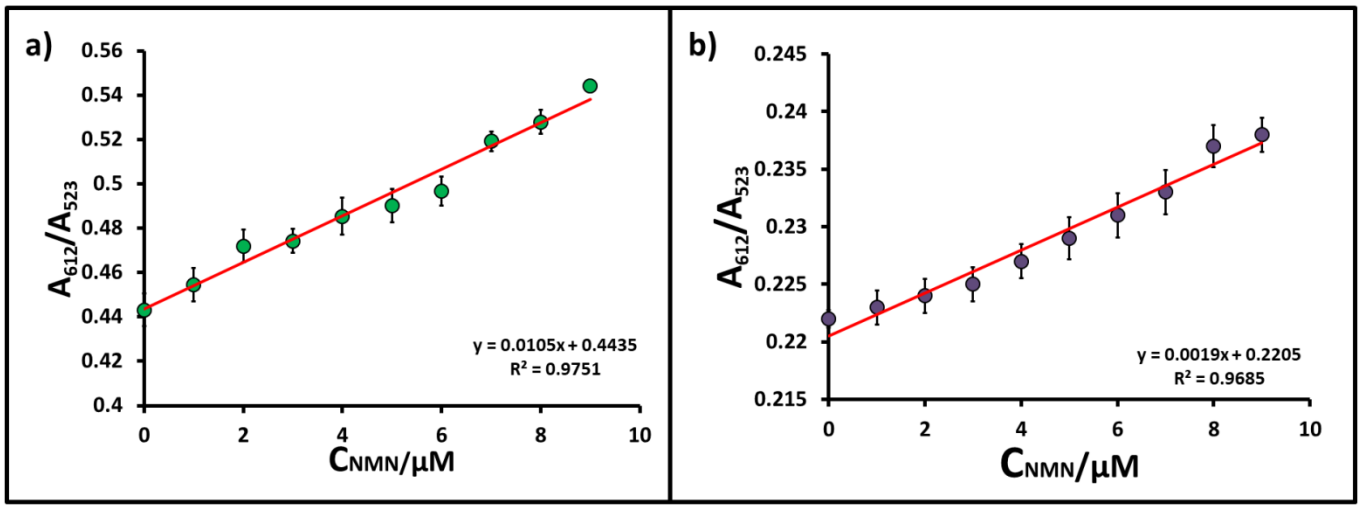

Figure 5. Plots of A_{612}/A_{523} versus NMN concentration within the 0-10 µM range for: a) optimized probe **OGNP1**; and b) **GNP1**. Error bars correspond to the s. d. from three independent experiments.

*3.5 Evaluation of **OGNP1** sensitivity in urine*

In order to evaluate the sensing capabilities of **GNP1** in real samples, assays in synthetic urine were performed. **OGNP1** present a similar behaviour in urine [41] to that described above in aqueous media when increasing concentrations of NMN were added (Figure S7). From the A_{612}/A_{523} vs NMN concentration plots, a linear response in urine within the 0 to 10 µM NMN concentration range was observed, and a LOD of 0.52 µM was determined in

this medium, which was into the normal range for healthy adults in urine (0.15 to 3.05 μM) [40].

4. Conclusions

In conclusion, we present herein a simple, fast¸ selective and sensitive colorimetric method for the detection of normetanephrine, a pheochromocytoma-biomarker, using aqueous dispersions of spherical gold nanoparticles bifunctionalised with 4-(liponyloxy)benzaldehyde and *N*-acetylcysteine (**GNP1**). The presence of NMN induces the aggregation of the nanoparticles due to a double recognition process, which results in a clear colour change of the solution from red to blue, easily observed by naked eye, and a remarkable shift in the SPR band in the UV-vis spectrum. Selectivity essays in presence of other neurotransmitter metabolites such as homovanillic acid (HVA, a major catecholamine metabolite), 5-hydroxyindoleacetic acid (5-HIAA, a serotonin metabolite), and of other biomolecules present in urine such as glucose (Glc), uric acid (U.A), and urea, were performed. Only in the presence of NMN, a remarkable color change and UV-vis response was observed, demonstrating the high selectivity of the system. Regarding the sensitivity of the probe, a linear response within the 0-10 μM NMN concentration range and a LOD as low as 0.2 μM were determined in aqueous media with **OGNP1**. A similar response of the optimized probe to NMN was observed in synthetic urine, with a LOD of 0.52 μM. We think that probe **GNP1** can be a simple and effective alternative to determine NMN in aqueous media and urine, contributing to the early diagnosis of pheochromocytoma and paraganglioma tumours.

Acknowledgements

Financial support from the Spanish Government (project MAT2015-64139-C4) and the Generalitat Valencia (Project PROMETEOII/2014/047 and AICO/2017/093) is gratefully acknowledged. T. Godoy-Reyes is grateful to Generalitat Valenciana for her Santiago Grisolía fellowship. SCSIE (Universitat de València) is gratefully acknowledged for all the equipment employed.

Appendix A. Supplementary Data

Supplementary data associated with this article can be found, in the online version, at…

References

[1] G. Eisenhofer, J. W. Lenders, W. M. Linehan, M. M. Walther, D. S. Goldstein, and H. R. Keiser, Plasma normetanephrine and metanephrine for detecting pheochromocytoma in von Hippel–Lindau disease and multiple endocrine neoplasia type 2, N. Engl. J. Med. 340 (1999) 1872-1879.

[2] A. M. Sawka, R. Jaeschke, R. J. Singh, and W. F. Young Jr, A Comparison of Biochemical Tests for Pheochromocytoma: Measurement of Fractionated Plasma Metanephrines Compared with the Combination of 24-Hour Urinary Metanephrines and Catecholamines, J. Clin. Endocrinol. Metab. 88 (2003) 553-558.

[3] W. F. Young, Paragangliomas, Ann. N. Y. Acad. Sci. 1073 (2006) 21-29.

[4] G. Eisenhofer, H. Keiser, P. Friberg, E. Mezey, T. T. Huynh, B. Hiremagalur, T. Ellingson , S. Duddempudi, A. Eijsbouts and J. W. Lenders, Plasma Metanephrines Are Markers of Pheochromocytoma Produced by Catechol-O-Methyltransferase Within Tumors, J. Clin. Endocrinol. Metab. 83 (1998) 2175-2185.

[5] R. Därr, C. Pamporaki, M. Peitzsch, K. Miehle, A. Prejbisz, M. Peczkowska, D. Weismann, F. Beuschlein, R. Sinnott, S. R. Bornstein, H.P. Neumann, A. Januszewicz, J. Lenders, G. Eisenhofer. Biochemical diagnosis of phaeochromocytoma using plasma-free normetanephrine, metanephrine and methoxytyramine: importance of supine sampling under fasting conditions. Clin. Endocrinol. 80 (2014), 478-486.

[6] K. Pacak, W. M. Linehan, G. Eisenhofer, M. M. Walther, and D. S. Goldstein, Recent advances in genetics, diagnosis, localization, and treatment of pheochromocytoma, Ann. Intern. Med. 134 (2001) 315-329.

[7] R. El Khamlichi, D. Bouchta, M. B. Atia, M. Choukairi, R. T. Khalid, I. Raissouni, S. Tazi, A. Mohammadi, A. Soussi, K. Draoui, C. Faiza, M.L. Sefian, A novel carbon/chitosan paste electrode for electrochemical detection of normetanephrine in the urine, J Solid State Electrochem. 22 (2018) 1-12.

[8] S. Oishi, M. Sasaki, M. Masato, T. Sato, Urinary Normetanephrine and Metanephrine Measured by Radioimmunoassay for the Diagnosis of Pheochromocytoma: Utility of 24-Hour and Random 1-Hour Urine Determinations, J Clin Endocrinol Metab. 67 (1988) 614-618.

[9] E. Pussard, A. Chaouch, T. Said, Radioimmunoassay of free plasma metanephrines for the diagnosis of catecholamine-producing tumors, Clinical chemistry and laboratory medicine. 52 (2014) 437-444.

[10] B. G. Wolthers, I. P. Kema, M. Volmer, R. Wesemann, J. Westermann, B. Manz. Evaluation of urinary metanephrine and normetanephrine enzyme immunoassay (ELISA) kits by comparison with isotope dilution mass spectrometry, Clin. Chem. 43 (1997) 114-120.

[11] M. Y. Cheuk, Y. C. Lo, W. T. Poon, Determination of urine catecholamines and metanephrines by reversed-phase liquid chromatography-tandem mass spectrometry, Chin. J. Chromatogr. 35 (2017) 1042-1047.

[12] Zheng, J., Mandal, R., & Wishart, D. S. A sensitive, high-throughput LC-MS/MS method for measuring catecholamines in low volume serum, Anal. Chim. Acta. (2018) https://doi.org/10.1016/j.aca.2018.01.021

[13] R. T. Peaston, K. S. Graham, E. Chambers, J. C. van der Molen, S. Ball, Performance of plasma free metanephrines measured by liquid chromatography–tandem mass spectrometry in the diagnosis of pheochromocytoma, Clin. Chim. Acta. 411 (2010) 546-552.

[14] M. J. Whiting, Simultaneous measurement of urinary metanephrines and catecholamines by liquid chromatography with tandem mass spectrometric detection, Ann. Clin. Biochem. 46 (2009) 129-136.

[15] E. C. Y. Chan, P. Y. Wee, P. Y. Ho, P. C. Ho, High-performance liquid chromatographic assay for catecholamines and metanephrines using fluorimetric detection with pre-column 9-fluorenylmethyloxycarbonyl chloride derivatization, J Chromatogr B Biomed Sci Appl. 749 (2000) 179-189.

[16] G. P. Jackman, A simple method for the assay of urinary metanephrines using high performance liquid chromatography with fluorescence detection, Clin. Chim. Acta, 120 (1982) 137-142.

[17] B. H. Westerink, Determination of Normetanephrine, 3,4-Dihydroxyphenylethyleneglycol (Free and Total), and 3-Methoxy-4-Hydroxyphenylethyleneglycol (Free and Total) in Rat Brain by High-Performance Liquid Chromatography with Electrochemical Detection and Effects of Drugs on Regional Concentrations, J. Neurochem. 42 (1984) 934-942.

[18] P. Volin, Determination of urinary normetanephrine, metanephrine and 3-methoxytyramine by high-performance liquid chromatography with electrochemical detection: comparison between automated column-switching and manual dual-column sample purification methods, J Chromatogr B Biomed Sci Appl. 578 (1992) 165-174.

[19] J. J. Willemsen, C. F. Sweep, J. W. Lenders, H. A. Ross, Stability of plasma free metanephrines during collection and storage as assessed by an optimized HPLC method with electrochemical detection, Clin. Chem. 49 (2003) 1951.

[20] J. J. Pisano. A simple analysis for normetanephrine and metanephrine in urine. *Clin. Chim. Acta* 5 (1960), 406-414.

[21] R.N. Gupta, D. Price, P.M. Keane. Modified Pisano method for estimating urinary metanephrines. *Clin. Chem.* 19 (1973), 611–614.

[22] J-B. Corcuff, L. Chardon, I. H. Ridah, J. Brossaud. Urinary sampling for 5HIAA and metanephrines determination: revisiting the recommendations. Endocr. Connect. 6 (2017), R87-R98.

[23] K. Saha, S. S. Agasti, C. Kim, X. Li, V. M. Rotello, Gold nanoparticles in chemical and biological sensing, Chem. Rev. 112 (2012) 2739-2779.

[24] K. M. Mayer, J. H. Hafner, Localized surface plasmon resonance sensors, Chem. Rev. 111 (2011) 3828-3857.

[25] K. A. Rawat, J. R. Bhamore, R. K. Singhal, S. K. Kailasa, Microwave assisted synthesis of tyrosine protected gold nanoparticles for dual (colorimetric and fluorimetric) detection of spermine and spermidine in biological samples, Biosens. Bioelectron. 88 (2017) 71-77.

[26] A. Martí, A. M. Costero, P. Gaviña, M. Parra, Selective colorimetric NO (g) detection based on the use of modified gold nanoparticles using click chemistry, Chem. Commun. 51 (2015) 3077-3079.

[27] J. V. Rohit, S. K. Kailasa, Simple and selective detection of pendimethalin herbicide in water and food samples based on the aggregation of ractopamine-dithiocarbamate functionalized gold nanoparticles, Sens. Actuators B Chem. 245 (2017) 541-550.

[28] L. Chen, W. Lu, X. Wang, L. Chen, A highly selective and sensitive colorimetric sensor for iodide detection based on anti-aggregation of gold nanoparticles, Sens. Actuators B Chem. 182 (2013) 482-488.

[29] C. Agami, T. Rizk, Role of solvent on the diastereoselectivity of oxazolidine formation from (–)-ephedrine, J. Chem. Soc., Chem. Commun. 24 (1983) 1485-1486.

[30] H. Su, Q. Zheng and H. Li, Colorimetric detection and separation of chiral tyrosine based on N-acetyl-L-cysteine modified gold nanoparticles, J. Mater. Chem. 22 (2012) 6546-6548.

[31] T. M. Godoy-Reyes, A. Llopis-Lorente, A. M. Costero, F. Sancenón, P. Gaviña, and R. Martínez-Máñez, Selective and sensitive colorimetric detection of the neurotransmitter serotonin based on the aggregation of bifunctionalised gold nanoparticles, Sens. Actuators B Chem. 258 (2017) 829-835.

[32] P. Zhao, N. Li and D. Astruc, State of the art in gold nanoparticle synthesis, Coord. Chem. Rev. 257 (2013) 638-665.

[33] J. Turkevich, P. C. Stevenson and J. Hillier, A study of the nucleation and growth processes in the synthesis of colloidal gold, Discuss. Faraday Soc. 11 (1951) 55-75

[34] G. Frens, Controlled nucleation for the regulation of the particle size in monodisperse gold suspensions, Nature-Phys Sci. 241 (1973) 20-22.

[35] C. Zhang, G. Shen, Y. Shen, X. Zhang. The development of an electrochemical immunosensor using a thiol aromatic aldehyde and PAMAM-functionalized Fe3O4@Au nanoparticles. Anal. Biochem. 485 (2015), 66-71.

[36] W. Haiss, N. T. K. Thanh, J. Aveyard and D. G. Fernig, Determination of size and concentration of gold nanoparticles from UV− Vis spectra, Anal. Chem. 79 (2007) 4215-4221.

[37] S.-Y. Lin, Y.-T. Tsai, C.-C. Chen, C.-M. Lin and C.-H. Chen, Two-step functionalization of neutral and positively charged thiols onto citrate-stabilized Au nanoparticles, J. Phys. Chem. B. 108 (2004) 2134-2139.

[38] X. Liu, M. Atwater, J. Wang and Q. Huo, Extinction coefficient of gold nanoparticles with different sizes and different capping ligands, Colloids Surf. B. 58 (2007) 3-7.

[39] B. Kong, A. Zhu, Y. Luo, Y. Tian, Y. Yu, G. Shi. Sensitive and selective colorimetric visualization of cerebral dopamine based on double molecular recognition. Angew. Chem. 123 (2011) 1877-1880

[40] Mayo Clinic. (s.f.). Mayo medical laboratories. https://www.mayomedicallaboratories.com/testcatalog/Clinical+and+Interpretive/83006 , (accessed December2017).

[41] Cerilliant Analitycal Reference Standards, https://www.cerilliant.com/shoponline/Item_Details.aspx?itemno=1cedba31-c7f4-4ab1-ba9f-a02f3328d204&item=S-020, (accessed December2017).